RSC Advances

PAPER

View Article Online
View Journal | View Issue

Cite this: *RSC Adv.*, 2021, **11**, 18417

Facile synthesis of a carbon dots and silver nanoparticles (CDs/AgNPs) composite for antibacterial application†

Xinjing Wei, Feng Cheng, Yue Yao, Xiaotong Yi, Binxiao Wei, Hongbin Li, Yadong Wu and Jinmei He*

Received 2nd April 2021
Accepted 10th May 2021

DOI: 10.1039/d1ra02600c

rsc.li/rsc-advances

Bacterial infections can seriously harm human health, and the overuse of traditional antibiotics and antibacterial agents will increase the resistance of bacteria. Therefore, it is necessary to prepare a new kind of antibacterial material. In this work, a carbon dots and silver nanoparticles (CDs/AgNPs) composite has been synthesized in a one-step facile method without the introduction of toxic chemicals, wherein CDs could serve as a reducing and stabilizing agent. The CDs/AgNPs composite was characterized by UV-vis spectrophotometry, X-ray photoelectron spectroscopy (XPS), X-ray diffraction (XRD), and transmission electron microscopy (TEM), which demonstrate that the silver nanoparticles were successfully synthesized in the composite. The zeta potential of the CDs/AgNPs composite was −15.3 mV, indicating that the composite possesses high stability. Furthermore, the composite also exhibited biocidal effects for both Gram-negative *E. coli* bacteria and Gram-positive *S. aureus* bacteria. Thus, the composite is considered to be of great potential in bactericidal and biomedical applications.

Introduction

Since fluorescent carbon dots (CDs) were discovered by accident during the process of separating and purifying single walled carbon nanotubes in 2004, CDs have attracted tremendous attention around the world.[1,2] As we all know, many methods have been used to synthesize fluorescent CDs,[3] such as hydrothermal treatment,[4] thermal decomposition,[5] ultrasonic-microwave irradiation,[6] and chemical oxidation.[7] However, most of these methods usually require expensive energy-consuming equipment or large amounts of toxic chemicals, which means that the preparation process of CDs is complex and extremely difficult.[8] Therefore, it is of great importance to develop convenient and environmentally friendly methods for preparing fluorescent CDs. Subsequently, scientists have devoted effort to synthesizing fluorescent CDs using natural biomass as the precursor, such as grass,[9] coffee grounds,[10] sweet lemon peel,[11] garlic,[12] plant leaves,[13] and fruit juice.[14,15] This is due to the fact that natural biomass is not only abundant, sustainable and renewable, but also cheap, readily available and nontoxic. Generally speaking, the fluorescence performances of CDs are superior to conventional semiconductor quantum dots and organic fluorescent dyes, such as photo-stability, no bleaching and blinking fluorescence, and excitation-dependent emission fluorescence.[16] Furthermore, fluorescent CDs also have chemical stability, good aqueous solubility, low cytotoxicity, and high biocompatibility. Owing to these fascinating properties, CDs have been widely applied in fluorescence imaging,[17,18] fluorescence detection,[19] drug delivery[20] and catalysis.[21]

Recently, fluorescent CDs have been used to stabilize and reduce metal nanomaterials due to the abundant oxygen containing functional groups (hydroxyl, carbonyl, carboxyl and epoxy) on their surface, which were considered as an excellent electron acceptor and electron donor.[22–25] In particular, fluorescent CDs were selected as reducing and stabilizing agent, which can be used to synthesize silver nanoparticles (AgNPs) to improve antibacterial property. Specifically, silver nanoparticles have widely applied in many bactericidal applications against numerous bacteria and viruses.[26] Compared with most other antibacterial materials, including quaternary ammonium compounds, metal ions and antibiotics, silver nanoparticles have a higher bactericidal ability and a relatively lower cost, as well as they can slowly release silver ions to inactivate bacteria.[27–29] As we know, silver nanoparticles not only have antibacterial property, but also have hydrophilicity and negative surface charge. Moreover, CDs play an important role in reducing silver ions and stabilizing the nanoparticles, the addition of fluorescent CDs to silver nanoparticles can increase the negative surface charge and hydrophilicity.[30] Meanwhile, the fluorescent CDs could be quenched by silver nanoparticles due to their proximity, resulting in surface plasmon enhanced energy transfer from CDs to AgNPs.[31] Currently, a great deal of

MIIT Key Laboratory of Critical Materials Technology for New Energy Conversion and Storage, School of Chemistry and Chemical Engineering, Harbin Institute of Technology, Harbin 150001, People's Republic of China. E-mail: hejinmei@hit.edu.cn; Fax: +86-0451-8641-4806; Tel: +86-0451-8641-4806

† Electronic supplementary information (ESI) available. See DOI: 10.1039/d1ra02600c

effort has been put into the synthetic process of CDs/AgNPs composite, however, a series of reducing agents, such as sodium borohydride, sodium citrate, citric acid and so on, are still used to assist in reducing silver ions.[22,32,33] This makes the process complex and toxic, so it should be interesting to obtain CDs/AgNPs composite by a facile and friendly method.[34]

In this work, fluorescent carbon dots derived from natural *Gynostemma* were synthesized through a facile pyrolysis method without the introduction of toxic chemicals. This synthetic method of CDs was more environment-friendly than that of other reports. And then in the typical process, silver nitrate solution was added to the CDs solution without any additional reducing agents, silver nanoparticles could be grown and attached with CDs by heating a mixture of Ag ions and CDs solution. The fluorescence emission was effectively quenched, and the CDs/AgNPs composite would be obtained. Subsequently, the synthesized CDs/AgNPs composite was thoroughly characterized by important analytical instruments. And the antibacterial activity of CDs/AgNPs composite has been evaluated by Gram-negative *E. coli* bacteria and Gram-positive *S. aureus* bacteria.

Experimental

Materials

The *Gynostemma* was bought at the drugstore, Heilongjiang, China. Silver nitrate ($AgNO_3$) was bought from Tianjin Beilian Chemical Technology Co, Ltd. All other chemical reagents were of analytical grade and could be used without further purification.

Preparation of carbon dots (CDs)

Carbon dots (CDs) were facilely synthesized from natural *Gynostemma* using pyrolysis method according to modify our previous work.[35] Briefly, the *Gynostemma* powder was collected from the grinding machine and then pyrolyzed at 400 °C under the nitrogen atmosphere. After four hours of heating, the black powder was cooled down at room temperature and then dispersed into water with continuous magnetically stirring. Subsequently, the black solution was filtrated through 0.22 μm filtration membrane to remove extra large particles. Finally, the solution was lyophilized under a vacuum condition to obtain the CDs powder.

Preparation of carbon dots and silver (CDs/AgNPs) composite

The CDs/AgNPs composite was prepared in a facile green method without adding any toxic chemicals. Typically, 10 mg of CDs powder was dissolved in distilled water with continuous magnetically stirring and boiled to 100 °C. Then, 10 mM $AgNO_3$ was added into the CDs solution and stirred for 60 min under dark condition. Afterwards, the solution was centrifuged at 11 000 rpm for 10 min, and the CDs/AgNPs composite was washed by distilled water three times to remove extra silver nitrate and CDs. Finally, CDs/AgNPs composite was collected by lyophilizing under a vacuum condition and kept at 4 °C for future use.

Characterizations

The fluorescence spectrum was recorded by a Varian Cary Eclipse fluorescence spectrophotometer with 1.0 cm path length quartz cuvette at room temperature. The UV-vis absorption spectrum was recorded by using the PerkinElmer LAMBDA XLS+ UV-vis spectrophotometer from 200 nm to 800 nm with 1.0 cm path length quartz cuvette. X-ray photoelectron spectroscopy (XPS) measurements were carried out on the Thermo Scientific Escalab250Xi surface analysis spectrometer. The X-ray diffraction (XRD) spectra were analysed by Empyrean X-ray diffractometer within the range of 10–90° (2θ). The zeta potential was measured by using a Malvern Zetasizer Nano ZS. The transmission electron microscopy (TEM) image was obtained with a JEM-2100F electron microscope, and the sample of TEM was prepared by dropping the suspension onto the carbon coated copper grid and dried in air.

Bacterial culture and inhibition zone test

The Gram-negative *E. coli* bacteria and Gram-positive *S. aureus* bacteria were cultured to evaluate the antibacterial activity of the CDs/AgNPs composite. At the same time, the filter paper diffusion method was used to investigate the antibacterial activity of CDs/AgNPs composite. Normally, both bacteria were cultivated in sterilized Luria-Broth (LB) medium kept in 37 °C with continuous shaking for overnight. Appropriate amount of bacterial suspension was evenly coated on the solid medium plates. And then a filter paper with 25 μL of sample (2.5 mg mL^{-1} and 5.0 mg mL^{-1}) was plated on the bacterial-coated solid medium plates. Then the solid medium plates were transferred in the 37 °C incubator for 18 h. Finally, the diameters of the inhibition zone were measured to investigate the antibacterial activity.

Results and discussion

The synthetic strategy of CDs/AgNPs composite by a green method was schematically illustrated in Scheme 1. Specifically, the fluorescent carbon dots were prepared by using natural *Gynostemma* as a green precursor *via* pyrolysis treatment. And then silver nitrate was added to the CDs solution with continuous stirring and heating. The silver ions were interacted with the oxygen containing functional groups on the surface of CDs, and CDs were used as stabilizer and reductant to reduce silver ions. Finally, the CDs/AgNPs composite was formed without any additional reducing agents.

The fluorescence emission spectrum of CDs solution has been shown in Fig. 1a, which embodied that the excitation dependent emission behaviour of CDs. When the excitation wavelength increasing from 300 nm to 400 nm, the emission

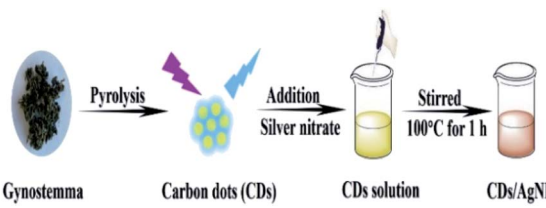

Scheme 1 The schematic illustration for the synthetic process of the CDs/AgNPs composite.

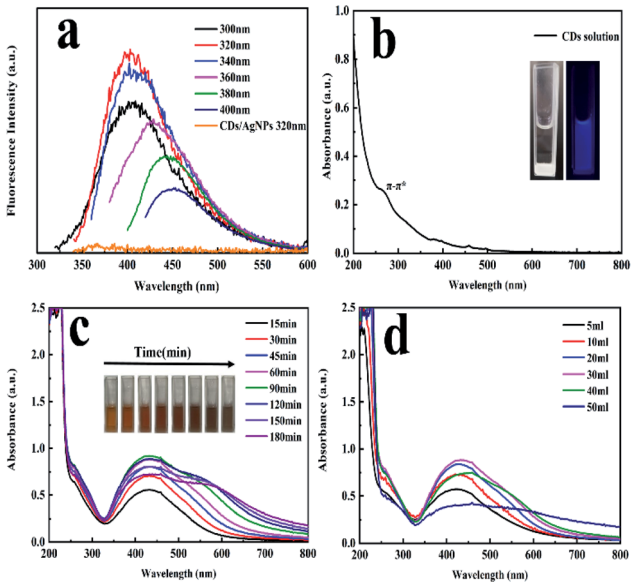

Fig. 1 (a) Fluorescence emission spectrum of CDs and CDs/AgNPs composite. (b) UV-vis absorption spectrum of CDs. Inset: photographs of CDs under sunlight (left) and UV light (right). UV-vis absorption spectrum during the synthesis of CDs/AgNPs composite. (c) Different reaction time and its photograph. (d) Different additive amount of silver nitrate.

peak also shifted from 400 nm to 450 nm. And the maximum emission peak at 400 nm occurred at the excitation wavelength of 320 nm. This characteristic might be attribute to the presence of diverse emissive sites on the surface of CDs.[35] However, it was also found that the CDs/AgNPs composite no longer have fluorescent emission peak under the excitation wavelength of 320 nm. This might be due to the silver ions interacted with the functional groups on the surface of CDs, and induced electron transfer between CDs and silver nanoparticles. In particular, the UV-vis absorption spectrum of the CDs solution in Fig. 1b had a typical absorption at about 270 nm, which was attributed to the π–π* electronic transition of C=C bonds of CDs. Moreover, the inset in Fig. 1b displayed a typical blue fluorescence of CDs under excitation of 365 nm UV light, and the CDs solution was transparent and light yellow under the sunlight. What's more, as shown in Fig. 1c and d, the UV-vis absorption spectrum of CDs/AgNPs composite exhibited a new strong absorption peak around 433 nm attributed to the surface plasmon resonance (SPR), which implied the successful formation of CDs/AgNPs composite.[36] Concretely, Fig. 1c represented the effect of reaction time on the synthesis of CDs/AgNPs composite. With the increase of time, the colour of the reaction solution changed obviously, and a wide absorption peak appeared at 550–600 nm. The wide absorption peak meant that the nanoparticles have aggregated, which may lead to larger particle sizes.[31] At the same time, when the silver nanoparticles got together in close proximity, the surface plasmon interacted to influence the resonant excitation, resulting in the colour variation from yellow to brown.[28] Thus, we chose to heat the mixture solution for 60 min to synthesize of CDs/AgNPs composite. Similarly, Fig. 1d represented the effect of the additive amount of silver nitrate on the synthesis of CDs/AgNPs composite. With the increase of the additive amount of silver nitrate, the absorption peak of silver nanoparticles gradually increased at 425–433 nm, but when the additive amount of silver nitrate exceeded 30 mL, the aggregation of silver nanoparticles was serious, resulting in the red shift of the absorption peak.[31] Finally, we added 30 mL silver nitrate solution (10 mM) into CDs solution to synthesize CDs/AgNPs composite by heating for 60 min.

Moreover, the XPS spectroscopy was carried out to investigate the elemental composition of the CDs/AgNPs composite as shown in Fig. 2. The XPS survey spectrum of CDs/AgNPs composite (Fig. 2a) comprise carbon, oxygen and silver elements at the binding energies of 284 eV, 531 eV and 368 eV, respectively. Then Fig. 2b–d showed the individual high resolution XPS spectrum for 1s splitting of carbon, oxygen and 3d splitting of silver. As given in Fig. 2b, the C 1s spectrum of CDs/AgNPs composite showed three main peaks with the binding energies at 284.6 eV, 285.72 eV, and 288.5 eV, which could be separately assigned to C–C (sp^3)/C=C (sp^2), C–O, and C=O groups, respectively. The deconvolution of O 1s spectrum in Fig. 2c appeared two peaks at 531.67 eV and 532.93 eV, which were attributed to C=O and C–O groups. In addition, as shown in Fig. 2d, the Ag 3d spectrum of CDs/AgNPs composite emerged two typical peaks at binding energy of 368.26 eV and 374.21 eV, corresponding to Ag $3d_{5/2}$ and Ag $3d_{3/2}$, respectively. It has been reported that the difference between two peaks was about 6 eV, indicating that the silver was exist as zero-valent silver nanoparticles in the composite.[27,36] Thus, the XPS analysis confirmed that the CDs/AgNPs composite had been synthesized successfully. Furthermore, the oxygen containing functional groups on the surface of CDs might take part to

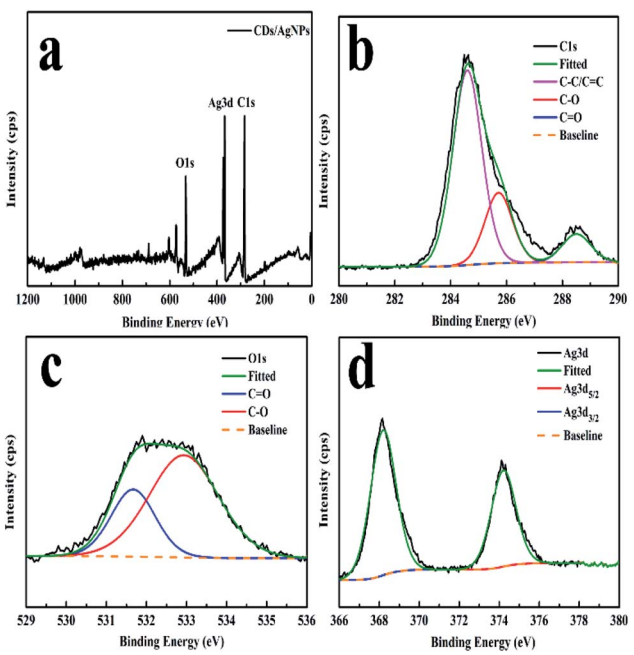

Fig. 2 XPS spectrum of the CDs/AgNPs composite. (a) The survey spectrum. (b) The C 1s spectrum. (c) The O 1s spectrum. (d) The Ag 3d spectrum.

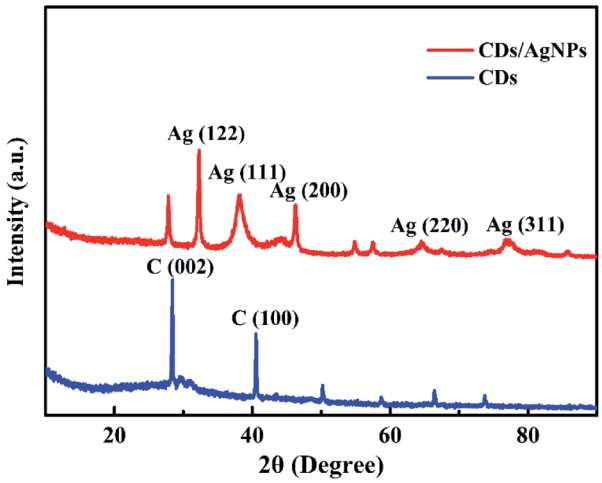

Fig. 3 XRD patterns of CDs and CDs/AgNPs composite.

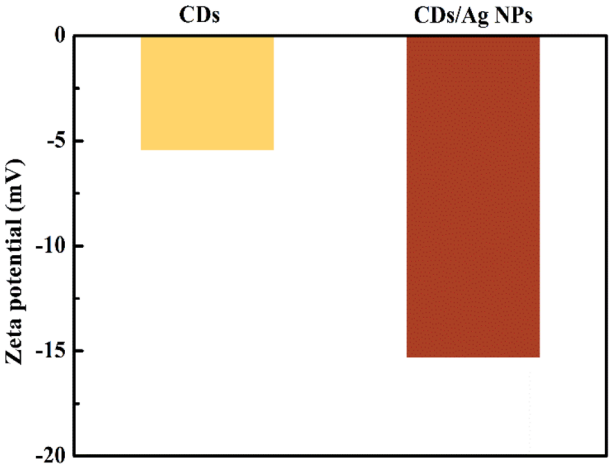

Fig. 4 Zeta potential of CDs and CDs/AgNPs composite.

reduce the silver ions to silver nanoparticles.[11,34] Due to the silver ions were attracted to the surface of CDs through electrostatic interaction with the oxygen containing functional groups, then the silver ions were reduced by CDs through electron transfer from the CDs to the silver ions. Compared with the C 1s spectrum of CDs (Fig. S1†), the intensity of C–O group peak was decreased and the intensity of C=O group peak was increased (Fig. 2b), which indicated that the C–O groups on the surface of CDs were oxidized and changed to C=O groups in the process of CDs/AgNPs composite formation.[37,38]

Additionally, the crystal structure of CDs/AgNPs composite was characterized by XRD. As shown in Fig. 3, the XRD pattern of CDs exhibited two main sharp peaks with the 2θ values of 28.5° and 40.7°, which related to the (002) and (100) planes of graphene and revealed the formation of CDs. Obviously, for the CDs/AgNPs composite, the peak corresponding to the (002) plane of graphene slightly shifted to 27.8°, which might be attributed to the interaction between silver nanoparticles and the CDs surface. And the significant peaks at 32.3°, 38.2°, 46.2°, 64.4°, 76.8° could be assigned to the (122), (111), (200), (220) and (311) planes of silver nanoparticles, respectively.[39] Thus, the XRD result confirmed the presence of CDs and silver nanoparticles in the CDs/AgNPs composite.

Furthermore, in order to identify the stability of the CDs/AgNPs composite, the zeta potential was carried out to measure the charge of CDs/AgNPs composite. The high negative value can produce repulsive force among CDs/AgNPs composite, resulting in stabilization of synthesized CDs/AgNPs composite.[40] As shown in Fig. 4, the zeta potential of CDs solution showed the value of −5.44 mV, while the zeta potential of CDs/AgNPs composite was −15.3 mV, indicating that the CDs/AgNPs composite possesses high stability.

Meanwhile, the morphology and size distribution of CDs/AgNPs composite was characterized by TEM. As shown in Fig. 5a and b, the CDs/AgNPs composite was spheroid and well dispersed, and the size distribution histogram showed a wide size distribution ranging from 7 nm to 20 nm, with the mean size around 13 nm. While the TEM image of CDs was showed in Fig. S2,† which indicated that CDs was dispersed and spherical in shape. The size distribution of CDs was between 1.6 nm and 3 nm with an average size of about 2.35 nm. It could be seen that the size of CDs/AgNPs composite particles were larger than that of CDs particles. Therefore, this meant that the CDs/AgNPs composite had been synthesized successfully.

The antibacterial activity of CDs/AgNPs composite against Gram-negative *E. coli* bacteria and Gram-positive *S. aureus* bacteria was investigated by the inhibition zone test. As shown in Fig. 6, it could be observed that treatment by PBS or CDs did not appear any inhibition zone for both *E. coli* and *S. aureus*

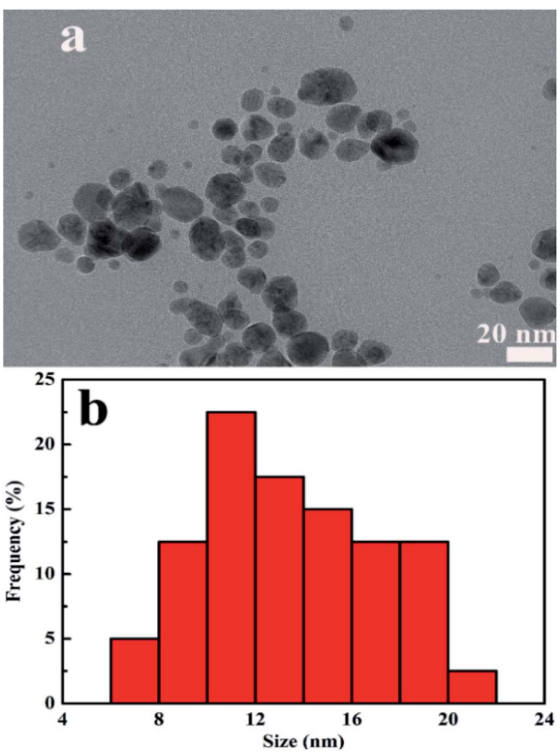

Fig. 5 (a) TEM image of CDs/AgNPs composite. (b) Particle size distribution histogram of CDs/AgNPs composite.

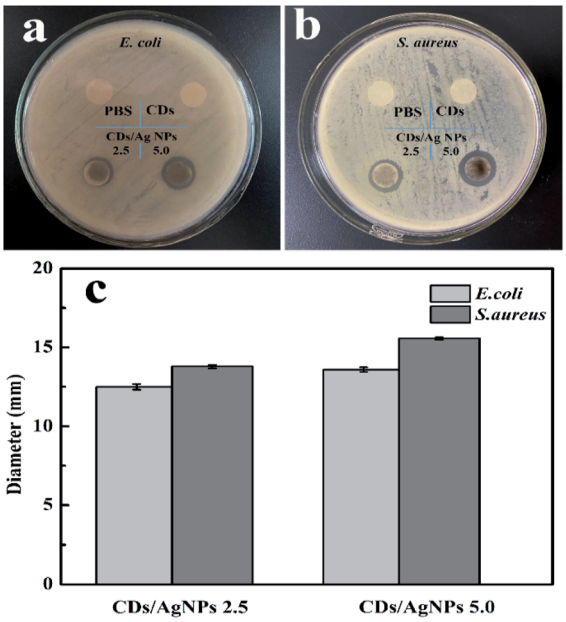

Fig. 6 The antibacterial effect of CDs/AgNPs composite. (a) Photograph of *E. coli* bacteria. (b) Photograph of *S. aureus* bacteria. (c) The inhibition zone of CDs/AgNPs composite.

bacteria. This meant that CDs alone had no antibacterial effect. However, it should be note that CDs/AgNPs composite clearly showed inhibition zone for both *E. coli* bacteria and *S. aureus* bacteria. And the diameters of inhibition zone of CDs/AgNPs composite were shown in the histogram, the diameters of inhibition zone of CDs/AgNPs composite towards *E. coli* bacteria was around 12–13 mm, the diameters of inhibition zone of CDs/AgNPs composite towards *S. aureus* bacteria was around 13–15 mm. This antibacterial effect of CDs/AgNPs composite was obviously superior to CDs. And the inhibition zone diameters of some reported antibacterial nanomaterials were summarized in Table S1.† Thus, the CDs/AgNPs composite have promising antibacterial effect against *E. coli* bacteria and *S. aureus* bacteria. In addition, the morphological changes of bacteria were observed by SEM before and after treated with CDs/AgNPs composite. As shown in Fig. S3,† the untreated bacteria were appeared an intact morphology and smooth surface, however, after treatment with CDs/AgNPs composite, the bacteria were deformed and fragmentated, resulting in the death of bacteria. Therefore, these CDs/AgNPs composite could be applied in antibacterial application.

Conclusions

In this study, the carbon dots and silver nanoparticles (CDs/AgNPs) composite has been synthesized in a one-step facile method without the introduction of toxic chemicals, wherein CDs could serve as a reducing and stabilizing agent. And the fluorescent CDs was obtained by the natural *Gynostemma* using pyrolysis method. The silver nanoparticles can be grown and attached with CDs by heating a mixture of Ag ions and CDs solution. The UV-vis absorption spectrum of CDs/AgNPs composite exhibited a new strong absorption peak around 433 nm attributed to the surface plasmon resonance, which implies the successful formation of silver nanoparticles in the CDs/AgNPs composite. At the same time, the XPS and XRD analysis also showed the characteristic peaks of the silver nanoparticles in the composite. And the zeta potential of CDs/AgNPs composite indicated that the composite possesses excellent stability. Meanwhile, the TEM image showed that the CDs/AgNPs composite was obtained with the average particle size around 13 nm. Furthermore, the composite also exhibited biocidal effect for both Gram-negative *E. coli* bacteria and Gram-positive *S. aureus* bacteria. Therefore, the CDs/AgNPs composite is considered to be of great potential in antibacterial and biomedical applications in the future.

Conflicts of interest

There are no conflicts to declare.

Acknowledgements

This work was financially supported by the National Natural Science Foundation of China (No. 51873048), National Natural Science Foundation of China (No. 22005077), Heilongjiang Postdoctoral Fund (No. LBH-Z20141), and National Natural Science Foundation of China (No. 51903066).

Notes and references

1 X. Y. Xu, R. Ray, Y. L. Gu, H. J. Ploehn, L. Gearheart, K. Raker and W. A. Scrivens, *J. Am. Chem. Soc.*, 2004, **126**, 12736–12737.
2 Y. R. Kumar, K. Deshmukh, K. K. Sadasivuni and S. K. K. Pasha, *RSC Adv.*, 2020, **10**, 23861–23898.
3 S. Tajik, Z. Dourandish, K. Zhang, H. Beitollahi, Q. V. Le, H. W. Jang and M. Shokouhimehr, *RSC Adv.*, 2020, **10**, 15406–15429.
4 A. A. Kajani, A. K. Bordbar, M. A. Mehrgardi, S. H. Zarkesh-Esfahani, H. Motaghi, M. Kardi, A. R. Khosropour, J. Ozdemir, M. Benamara and M. H. Beyzavi, *ACS Appl. Bio Mater.*, 2018, **1**, 1458–1467.
5 J. Wang, C. F. Wang and S. Chen, *Angew. Chem., Int. Ed.*, 2012, **51**, 9297–9301.
6 Y. Y. Yao, G. Gedda, W. M. Girma, C. L. Yen, Y. C. Ling and J. Y. Chang, *ACS Appl. Mater. Interfaces*, 2017, **9**, 13887–13899.
7 A. Suryawanshi, M. Biswal, D. Mhamane, R. Gokhale, S. Patil, D. Guin and S. Ogale, *Nanoscale*, 2014, **6**, 11664–11670.
8 X. Zhang, M. Jiang, N. Niu, Z. Chen, S. Li, S. Liu and J. Li, *ChemSusChem*, 2018, **11**, 11–24.
9 S. Liu, J. Q. Tian, L. Wang, Y. W. Zhang, X. Y. Qin, Y. L. Luo, A. M. Asiri, A. O. Al-Youbi and X. P. Sun, *Adv. Mater.*, 2012, **24**, 2037–2041.
10 P. C. Hsu, Z. Y. Shih, C. H. Lee and H. T. Chang, *Green Chem.*, 2012, **14**, 917–920.
11 K. Ghosal, S. Ghosh, D. Ghosh and K. Sarkar, *Int. J. Biol. Macromol.*, 2020, **162**, 1605–1615.

12 S. J. Zhao, M. H. Lan, X. Y. Zhu, H. T. Xue, T. W. Ng, X. M. Meng, C. S. Lee, P. F. Wang and W. J. Zhang, *ACS Appl. Mater. Interfaces*, 2015, **7**, 17054–17060.
13 L. L. Zhu, Y. J. Yin, C. F. Wang and S. Chen, *J. Mater. Chem. C*, 2013, **1**, 4925–4932.
14 H. Huang, Y. Xu, C. J. Tang, J. R. Chen, A. J. Wang and J. J. Feng, *New J. Chem.*, 2014, **38**, 784–789.
15 H. Ding, Y. Ji, J. S. Wei, Q. Y. Gao, Z. Y. Zhou and H. M. Xiong, *J. Mater. Chem. B*, 2017, **5**, 5272–5277.
16 W. Wang, H. Lai, Z. Cheng, H. Kang, Y. Wang, H. Zhang, J. Wang and Y. Liu, *J. Mater. Chem. B*, 2018, **6**, 7444–7450.
17 V. Ramanan, S. K. Thiyagarajan, K. Raji, R. Suresh, R. Sekar and P. Ramamurthy, *ACS Sustainable Chem. Eng.*, 2016, **4**, 4724–4731.
18 N. Wang, Y. T. Wang, T. T. Guo, T. Yang, M. L. Chen and J. H. Wang, *Biosens. Bioelectron.*, 2016, **85**, 68–75.
19 T. Boobalan, M. Sethupathi, N. Sengottuvelan, P. Kumar, P. Balaji, B. Gulyas, P. Padmanabhan, S. T. Selvan and A. Arun, *ACS Appl. Nano Mater.*, 2020, **3**, 5910–5919.
20 N. Sarkar, G. Sahoo, R. Das, G. Prusty and S. K. Swain, *Eur. J. Pharm. Sci.*, 2017, **109**, 359–371.
21 M. Jayanthi, S. Megarajan, S. B. Subramaniyan, R. K. Kamlekar and V. Anbazhagan, *J. Mol. Liq.*, 2019, **278**, 175–182.
22 J. L. Ma, B. C. Yin, X. Wu and B. C. Ye, *Anal. Chem.*, 2017, **89**, 1323–1328.
23 A. Thakur, P. Kumar, D. Kaur, N. Devunuri, R. K. Sinha and P. Devi, *RSC Adv.*, 2020, **10**, 8941–8948.
24 W. F. Chen, J. L. Shen, S. N. Chen, J. Y. Yan, N. N. Zhang, K. B. Zheng and X. Liu, *RSC Adv.*, 2019, **9**, 21215–21219.
25 Y. Zhuo, D. Zhong, H. Miao and X. M. Yang, *RSC Adv.*, 2015, **5**, 32669–32674.
26 H. Y. Fang, W. M. Huang and D. H. Chen, *Nanotechnology*, 2019, **30**, 365603.
27 S. Kadian, G. Manik, N. Das, P. Nehra, R. P. Chauhan and P. Roy, *J. Mater. Chem. B*, 2020, **8**, 3028–3037.
28 F. Jalilian, A. Chahardoli, K. Sadrjavadi, A. Fattahi and Y. Shokoohinia, *Adv. Powder Technol.*, 2020, **31**, 1323–1332.
29 J. C. Jin, Z. Q. Xu, H. F. Zou, Z. Q. Zhou, Q. Q. Yang, B. B. Wang, F. L. Jiang and Y. Liu, *RSC Adv.*, 2016, **6**, 76989–76995.
30 A. Verma, S. Shivalkar, M. P. Sk, S. K. Samanta and A. K. Sahoo, *Nanotechnology*, 2020, **31**, 405704.
31 J. C. Jin, Z. Q. Xu, P. Dong, L. Lai, J. Y. Lan, F. L. Jiang and Y. Liu, *Carbon*, 2015, **94**, 129–141.
32 S. Han, H. Zhang, Y. J. Xie, L. L. Liu, C. F. Shan, X. K. Li, W. S. Liu and Y. Tang, *Appl. Surf. Sci.*, 2015, **328**, 368–373.
33 J. Y. Gan, W. C. Chong, L. C. Sim, C. H. Koo, Y. L. Pang, E. Mahmoudi and A. W. Mohammad, *Membranes*, 2020, **10**, 175.
34 Y. B. Su, B. F. Shi, S. Q. Liao, J. J. Zhao, L. N. Chen and S. L. Zhao, *ACS Sustainable Chem. Eng.*, 2016, **4**, 1728–1735.
35 X. J. Wei, L. Li, J. L. Liu, L. D. Yu, H. B. Li, F. Cheng, X. T. Yi, J. M. He and B. S. Li, *ACS Appl. Mater. Interfaces*, 2019, **11**, 9832–9840.
36 H. X. Ji, S. N. Zhou, Y. Fu, Y. Y. Wang, J. Y. Mi, T. C. Lu, X. R. Wang and C. L. Lu, *Mater. Sci. Eng., C*, 2020, **110**, 110735.
37 B. F. Shi, Y. B. Su, J. J. Zhao, R. J. Liu, Y. Zhao and S. L. Zhao, *Nanoscale*, 2015, **7**, 17350–17358.
38 S. Chen, X. Hai, X. W. Chen and J. H. Wang, *Anal. Chem.*, 2014, **86**, 6689–6694.
39 Y. Tian, F. L. Wang, Y. X. Liu, F. Pang and X. Zhang, *Electrochim. Acta*, 2014, **146**, 646–653.
40 T. Dutta, N. N. Ghosh, M. Das, R. Adhikary, V. Mandal and A. P. Chattopadhyay, *J. Environ. Chem. Eng.*, 2020, **8**, 104019.